THE ROLE OF INERT GAS EXCHANGE AND POPULATION STATISTICS IN STUDIES OF DECOMPRESSION SICKNESS

Richard G. Buckles, et al

Naval Medical Research Institute
Bethesda, Maryland

1973

UNCLASSIFIED

Security Classification

AD/A-004667

DOCUMENT CONTROL DATA - R & D

(Security classification of title, body of abstract and indexing annotation must be entered when the overall report is classified)

ORIGINATING ACTIVITY (Corporate author) NAVAL MEDICAL RESEARCH INSTITUTE BETHESDA, MARYLAND 20014	2a. REPORT SECURITY CLASSIFICATION UNCLASSIFIED 2b. GROUP

3. REPORT TITLE

THE ROLE OF INERT GAS EXCHANGE AND POPULATION STATISTICS IN STUDIES OF DECOMPRESSION SICKNESS

4. DESCRIPTIVE NOTES (Type of report and inclusive dates)

MEDICAL RESEARCH PROGRESS REPORT

5. AUTHOR(S) (First name, middle initial, last name)

RICHARD G. BUCKLES and E. HARDENBERGH

6. REPORT DATE	7a. TOTAL NO. OF PAGES	7b. NO. OF REFS
1973	34	13

8a. CONTRACT OR GRANT NO.	9a. ORIGINATOR'S REPORT NUMBER(S)
b. PROJECT NO.	M4306.01-1020 Report No. 1
c.	9b. OTHER REPORT NO(S) (Any other numbers that may be assigned this report)
d.	

10. DISTRIBUTION STATEMENT

THIS DOCUMENT HAS BEEN APPROVED FOR PUBLIC RELEASE AND SALE: ITS DISTRIBUTION IS UNLIMITED

11. SUPPLEMENTARY NOTES	12. SPONSORING MILITARY ACTIVITY
Reprinted from Chemical Engineering in Medicine, Washington, D.C. American Chemical Society, 1973	BUREAU OF MEDICINE AND SURGERY (NAVY) WASHINGTON, D.C. 20372

13. ABSTRACT Mass transfer models were combined with dose-response analysis to yield more insight into the fundamental etiology of decompression sickness. Data are presented that would favor a four-tissue model of a amster from an inert gas exchange point of view: (1) lung, (2 a fast tissue with a time constant corresponding to the cardiac output per gram of tissue, and (3,4) two slow tissues (time constant 6.3 and 25.5 min) corresponding to those tissue sites susceptible to bubble nuclea_ion.

I

DD FORM 1473 (PAGE 1)

S/N 0102-014-6600

UNCLASSIFIED

Security Classification

22

14. KEY WORDS	LINK A		LINK B		LINK C	
	ROLE	WT	ROLE	WT	ROLE	WT
1. Decompression sickness						
2. Hamsters						
3. Disease models-animals						

The Role of Inert Gas Exchange and Population Statistics in Studies of Decompression Sickness

RICHARD C. BUCKLES

Alza Research, 2631 Hanover St., Palo Alto, Calif. 94304

E. HARDENBERGH

Naval Medical Research Institute, National Naval Medical Center, Bethesda, Md. 20014

Mass transfer models were combined with dose–response analyses to yield more insight into the fundamental etiology of decompression sickness. Data are presented that would favor a four-tissue model of a hamster from an inert gas exchange point of view: (1) lung, (2) a fast tissue with a time constant corresponding to the cardiac output per gram of tissue, and (3, 4) two slow tissues (time constant 6.3 and 25.5 min) corresponding to those tissue sites susceptible to bubble nucleation.

Decompression sickness is a disease experienced by divers and airplane pilots. It can be avoided if one uses procedures based upon a mass transfer analysis. This type of analysis is very old, having been first carried out by Haldane *et al.* in 1908 (*1*). Recent modifications can only be viewed as empirical curve-fitting attempts based on an increased amount of data (*2*).

The studies reported here are oriented toward enunciating the basic mechanisms of the disease rather than improving the existing model by curve fitting. Because the population response to the disease exhibits wide variance, the dose–response characteristics of the animal must be incorporated into the model. This blending of pharmacokinetic models and dose–response models provides more insight into the etiology of the disease than has been available.

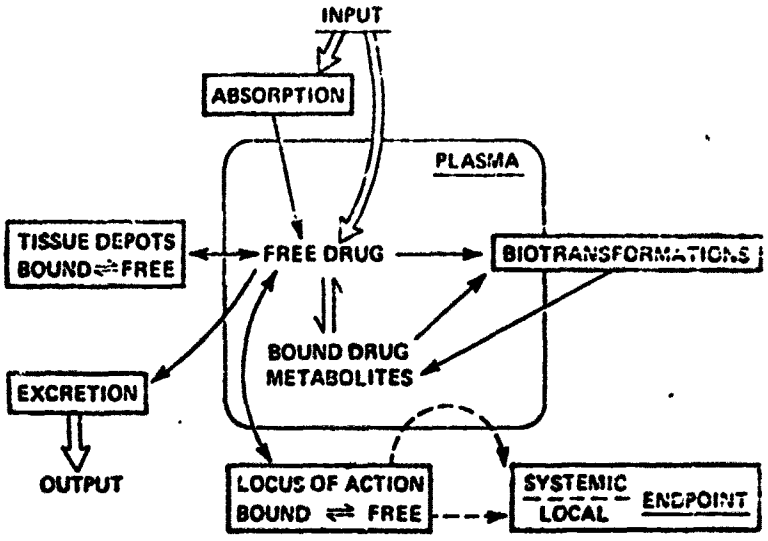

Figure 1. Drug distribution dynamics—i.e., many processes can act on a drug from its point of input into the body to its output. Possible responses to the drug are also shown, indicating their (often) indirect relationship to the drug.

Figure 1 summarizes the pharmacodynamacist's view of the flow of a material throughout the body from input to output, leading to a clinical endpoint. Through physiological measurements we can describe the transport of the material from input to the locus of action. We cannot confirm this process in decompression sickness because the locus is buried in peripheral tissue. Therefore, we must describe the population response (*i.e.*, endpoint) and make inferences about the process that occurs at the locus of action.

Decompression sickness represents the following simplifications of the general picture in Figure 1:

(1) The diffusing molecule is not protein bound.
(2) Time and dose are interrelated.
(3) Single route of introduction and excretion (the same route).
(4) No biotransformations occur.
(5) The locus of action is peripheral but random in location.

Since the action of the "drug" is a physical phenomena amenable to to mathematical description (*see* below), we hope that knowledge gained about the etiology of this disease in small animals can be scaled to larger animals and perhaps even to humans. The recent success of Bischoff *et al.* (3) in this type of scaling procedure for methadone provides increased confidence in the potential for applying the same scaling principles to decompression sickness.

Decompression Sickness

The symptoms of decompression sickness occur when bubbles form, grow, and circulate in the blood. The bubbles are generated when man goes from a high pressure to a low pressure environment, breathing some form of oxygen and "inert" gas. The inert gas is dissolved in all body tissues to a lesser or greater extent. (It is conventional to speak of the inert gas partial pressure, rather than its concentration, in these tissues [$P_{i\text{-tissue}} = C_{i\text{-tissue}} \div \alpha$]). When the hydrostatic pressure surrounding the animal is less than the partial pressure of the inert gas in any given tissue, there is a finite likelihood that nucleation of bubbles will occur, reducing the state of supersaturation in that tissue but leaving the tissue filled with bubbles. Divers enter this state of risk by breathing air at increased pressures while they are diving. They continue to absorb inert gas in various tissues while they are on the bottom. It is possible for divers to vary both the pressure and time of diving and end up with the same degree of risk. Because there has never been a satisfactory animal model for this disease, studies have been carried out on volunteer humans in simulated diving environments within steel chambers.

In 1966 experimental studies were initiated on the susceptibility of anaesthetized hamsters to decompression insult, attempting to utilize existing pharmacokinetic and toxicological modeling techniques to characterize the role of the inert gas in producing decompression sickness. The hamster model consisted of three discrete elements. First, a mass transfer model had to be developed that would describe the uptake,

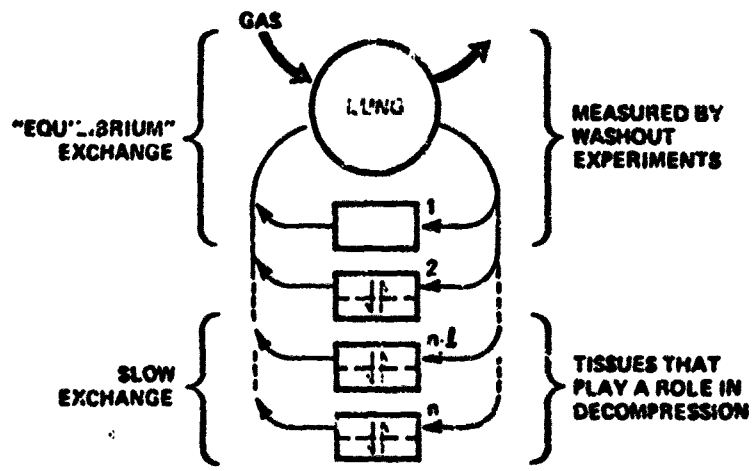

Figure 2. Generalized mass transfer model for the hamster
The model consists of n tissues, l of which play a role in initiating decompression sickness. The first few tissues equilibrate with the rapidly circulating blood and have a high water content. The slower tissues may be characterized by two compartments coupled by inert gas diffusion.

distribution, and elimination of nitrogen during exposure to high pressure air and a subsequent return to normal pressure. Secondly, the model had to take into account the response of the animal to supersaturation (*i.e., in vivo* nucleation had to be modeled). Finally, a population distribution based on the kinetics of bubble formation and growth would have to be superimposed upon the population response to bubbles.

Figure 2 describes the generalized mass transfer model based on the early work of Haldane (*1*). The region consisting of the lung and the fast tissue (No. 1) can be characterized by mass transfer studies of inert gas absorption and elimination. In these, it is assumed that Tissue 1 acts as a well-stirred chemical reactor so that the venous partial pressure of gas is equal to the average value for the tissue as a whole.

Somewhere in this model composed of *n* discrete tissues, it is postulated that the disease can be initiated by bubbles forming and growing. Evidence is presented here to indicate that it is the slow transport-limited tissues of the body that represent the tissues in which bubbles first nucleate. Mass transfer modeling of this sort postulates such tissues and then seeks experimental validation of their existence.

The population distribution elements of this model are described in Figure 3. Those distributions responding to a particular endpoint are plotted as a function of the inert gas tension in a characteristic tissue. This response would occur in an animal that had been exposed to a high pressure and then returned directly to 1 atm. Bubble formation begins when the tissue tension exceeds some lower limit and the population is

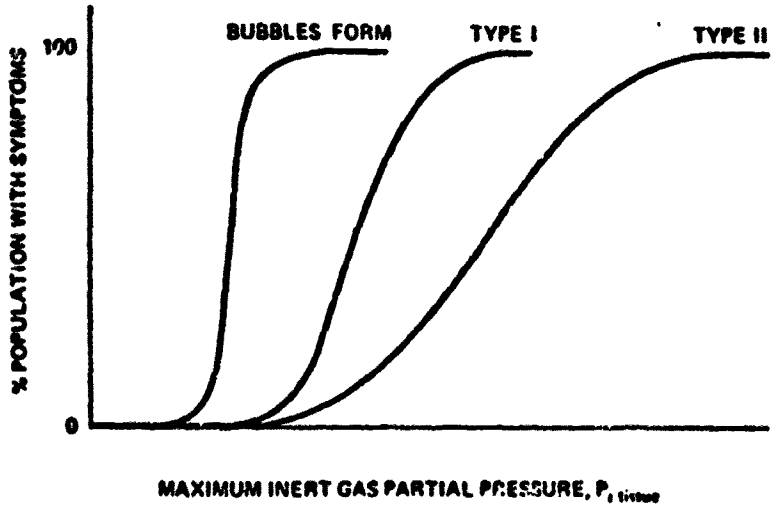

Figure 3. Generalized dose–response curves for decompression sickness *As the tissue partial pressure ($P_{t\,tissue}$) increases, the percentage of the population that exhibits a particular endpoint increases. The relative location of these three curves is the basis for much of the current controversy about modern diving practices.*

THIS
PAGE
IS
MISSING
IN
ORIGINAL
DOCUMENT

Care" prepared by the Committee on the Guide for Laboratory Animal Resources, National Academy of Sciences—National Research Council.

Our studies were carried out on male hamsters obtained from the NIH Breeding Colony, Bethesda, Md. They were anaesthetized with a chloralose urethane anaesthesia (1 cc/100 grams hamster with a solution containing 10 mg/cc chloralose, 10 mg/cc sodium [illegible], and 150 mg/cc urethane). Supplemental doses of 1/3 original dose were often required for long studies. The animals were kept a minimum of two weeks to stabilize dietary and environmental factors. An endotracheal tube, size PE60 or 90, was used in all cases, partly to eliminate the difficulty of respiratory stress, but more importantly in the gas washout studies to connect the animal directly to the breathing gas system.

Results

Two types of studies were carried out: the first, reported on a preliminary basis (*8*), involves the use of an endpoint—death—and is oriented towards the articulation of the receptor sites for bubble nucleation. The second study, reported here for the first time, involves a measurement of the fast inert gas exchange constants of the animal model. Both studies utilized air as a breathing mixture and were begun with the animal assumed to be in equilibrium with air at 1 atm ($P_{X_2} = 0.79$ atm).

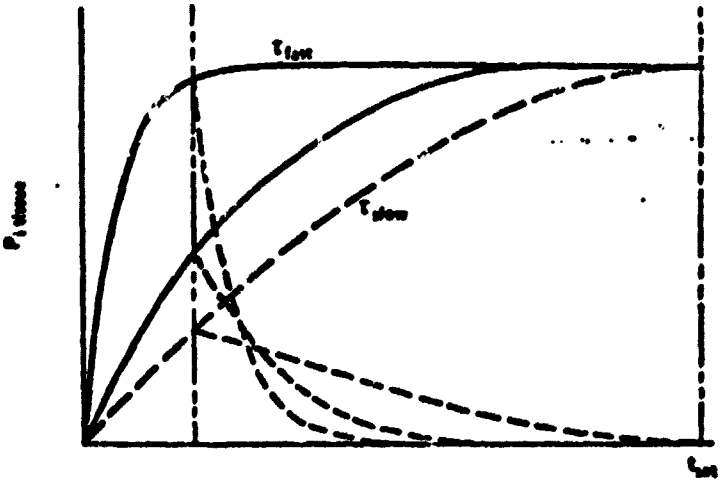

Figure 5. Inert gas partial pressure in the spectrum of hamster tissues during a simulated dive

The fast tissues (characterized by short time constants, τ_{fast}) rise rapidly to a level in equilibrium with the inspired air. In short dives, these tissues will be relatively more saturated than the slower ones (τ_{slow}). As the bottom time increases, the tissue partial pressures approach one another.

Dose–Response Curves. When the hamster is exposed to high ambient pressure, the partial pressure of nitrogen in its body tissues rises

along some form of exponential curve, ultimately reaching saturation (Figure 5). If at any time during this procedure the pressure is returned to 1 atm, the various body tissues are supersaturated with respect to ambient pressure and will attempt to return to ambient conditions (0.79 atm) along an exponential curve similar to that which they followed during the uptake portion of the dive. Short dives are characterized by high inert gas partial pressures in the tissues, represented by short time constants (τ_{fast}). However, long bottom time dives that show an ever-increasing degree of mortality, must reflect the gas uptake in the tissues with long-time constants (τ_{slow}).

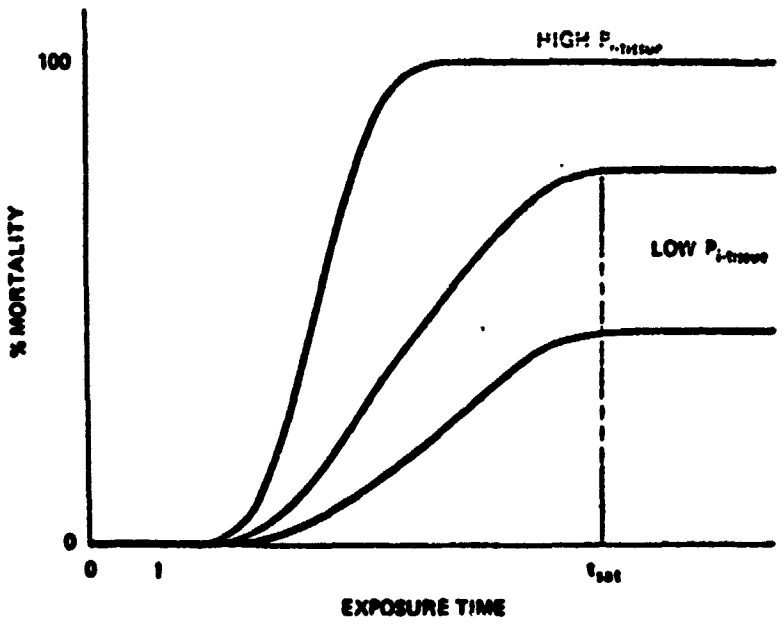

Figure 6. Generalized hamster dose–response curves
If the nitrogen partial pressure is high enough, the mortality will eventually go to 100%. However, with lower partial pressures the mortality rises to some asymptotic value after a constant time period. In this domain one can study the time effects independent of the nitrogen partial pressure.

Figure 6 shows three postulated dose–response curves that could be expected. In the curve marked high $P_{i\text{-}tissue}$, the ultimate response is 100% mortality because the inert gas partial pressure was so high that all animals were afflicted. If the depth of the dive is lowered (curves marked low $P_{i\text{-}tissue}$), the curve shifts to the right (towards increased exposure time) and flattens at a time (t_{sat}). In this range of pressures it is assumed that the time response is independent of the absolute pressure of the dive. Experiments of this kind are called time-based experiments (TB), and are used to characterize τ_{slow}, as defined in Figure 5.

Once τ_{slow} is determined, one may design an experimental dive sequence in which τ_{slow} will be the controlling tissue, regardless of depth. In these pressure-based trials (PB), one increases the absolute depth of the dive while maintaining the bottom time constant. An experimental dose–response curve similar to Figure 4 is then obtained and may be analyzed solely in terms of $P_{\ell\text{-tissue}}$, independent of time. $P_{\ell\text{-tissue}}$ can be calculated if one knows τ_{slow} and the time and pressure of a particular dive.

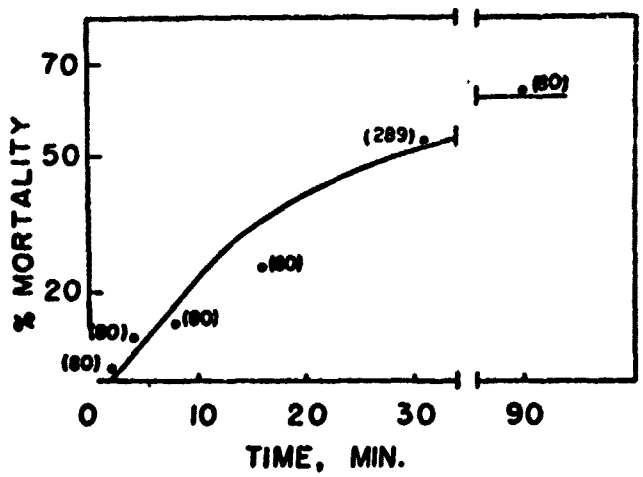

Figure 7. Hamster mortality as a function of time (8) The hamsters were exposed to 11.2 ata of air for varying tissues. This graph exhibits the experimental results and the "best" line estimate of a normal mortality curve for the data. The numbers in parentheses indicate sample size

The time-based and pressure-based studies were carried out in a small experimental chamber (*8*). The experimental results (% mortality as a function of time or pressure) were analyzed by the methods of probit analysis presented by Finney (*9*). The time-based studies were analyzed first (*see* Appendix I). A statistical best fit was applied to the data once it had been determined that the percent mortality that occurred at the longest bottom time (90 minutes) was the same as at the saturation level (*see* Figure 7). From the statistically best fit line of percent mortality *vs.* bottom time, the time associated with a mortality corresponding to 99% of saturation mortality was determined. Assuming that τ_{slow} characterizes a tissue that rises exponentially towards saturation, one may show that the time constant, τ_{slow}, is a simple multiple of the time to reach 99% of saturation (called t_{99}). From these experiments it was determined that $\tau_{slow} \simeq 25.5$ minutes.

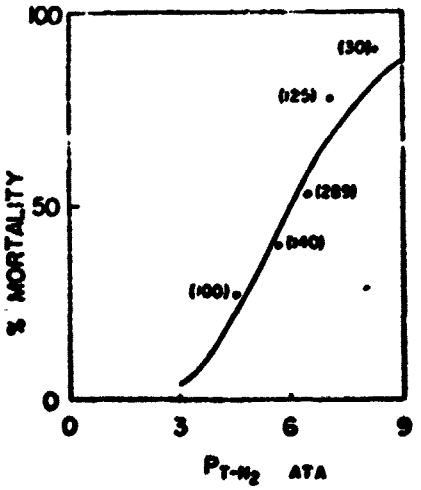

International Congress on Hyperbaric Medicine

Figure 8. Hamster mortality as a function of maximum value of slow tissue nitrogen partial pressure (8)
The dives were carried out for 31 min in air (F = 0.79 atm) and are related to the (assumed) P_{T-N_2} in the slowest tissue (τ_1 = 25.5 min). The partial pressure is related to dive depth, $P_{b,a}$, by:

$$P_{T-N_2} = 0.79 + F(P_{b,a} - 1)(1 - e^{-t/\tau_1})$$

The numbers in parentheses indicate the sample size.

The pressure-based data were carried out by diving to increasing depths with a bottom time of 31 minutes. This time was determined from τ_{slow} so that the tissue controlling the mortality incidence would be the slowest tissue (τ_{slow}) under all conditions. Figure 8 is a plot of the percent mortality *vs.* the inert gas tissue tension in the slowest tissue for these PB data.

One may compute the inert gas tissue tension in the slow tissue at the end of the shorter bottom time dives in the TB series. These data points are plotted on Figure 9 where they are superimposed on the data from Figure 8. The dives corresponding to 2, 4, and 8 minutes fall significantly above the best fit curve based on the PB data.

Nitrogen Washout Curves. These studies were carried out to ascertain directly the rate of nitrogen elimination in anaesthetized hamsters at 1 atm. Hamsters that were initially equilibrated with air were attached to a breathing circuit, shown in Figure 10, through which an 80/20 helium oxygen gas mixture was passed at a constant flow rate. The gas passed through a sampling valve of a gas chromatograph so that one could take discrete samples at fixed intervals after the animal was at-

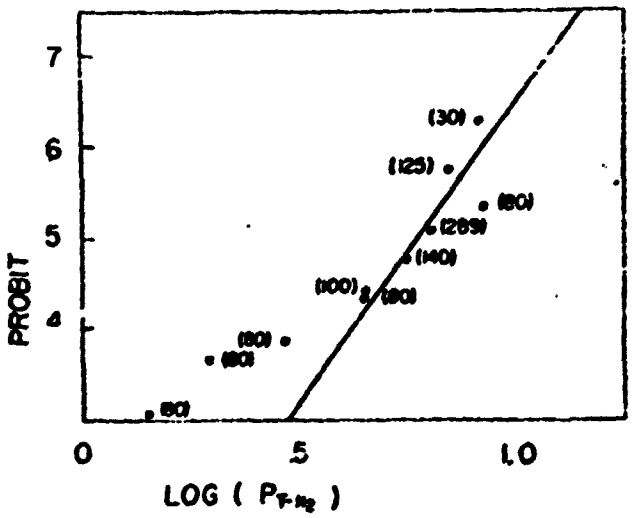

International Congress on Hyperbaric Medicine

Figure 9. Hamster mortality as a function of $P_{T\text{-}N_2}$ (8) The data are plotted (for illustration) as the probit vs. log $P_{T\text{-}N_2}$. The value of $P_{T\text{-}N_2}$ is computed from $P_{a,t}$ as in Figure 9, assuming $\tau = 25.5$ min. The solid line corresponds to a least-squares fit of the PB data. The TB data (□) fall significantly to the left of the line. The numbers in parentheses indicate the sample size (see Figure 8).

tached to the system. Since the system could be calibrated with known gases, the acquired data were expressed in terms of nitrogen fraction (F) at discrete times during the washout. The dead space between the animal connection and the sampling loop was negligible.

The method of data analysis is derived in Appendix II. The animals were grouped according to weight, and the average data were plotted in terms of the log $[F\dot{Q}/W]$ as a function of time. The experimental parameters measured were nitrogen fraction (F), gas flow rate ($\dot{Q}$), and hamster weight (W). Figure 11 is a characteristic curve. Nitrogen excretion decreased rapidly during the first two minutes (pulmonary washout) and then more slowly. A best-fit line was drawn by eye, and the slope and intercept of that line were determined. Table I is a list of the intercept and slope (F_0 and τ).

A mass balance on nitrogen shows that

$$K = \frac{f_{I}\alpha_{I}}{\alpha f} + f_{v}\alpha_{v}$$

where K is the ratio of total initial dissolved nitrogen to body weight. To determine K *a priori*, one must know the solubility coefficients for N_2

APPARATUS FOR
INERT GAS WASHOUT EXPERIMENTS

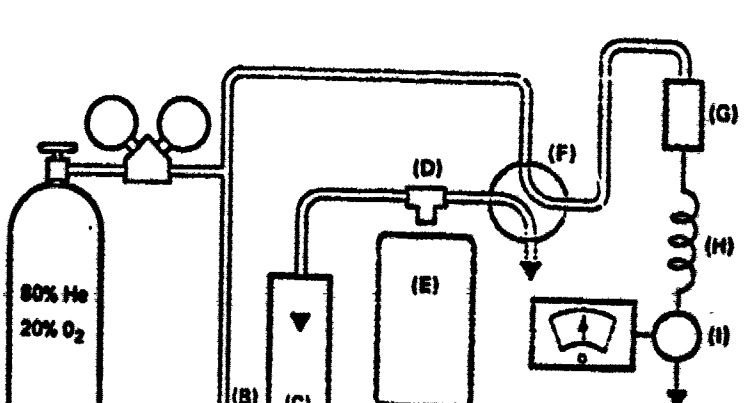

Figure 10. Hamster breathing loop for analysis of exhaled N_2. The system consists of: (a) compressed gas (80/20 He/O_2) and appropriate flow regulators; (b) fine flow rate control value; (c) rotometer; (d) T-joint with gas tight fitting for attaching hamster endotracheal tube; (e) heating pallet for hamster; (f) chromatograph sampling valve; (g) water and CO_2 absorbent bed; (h) chromatograph column; (i) thermal conductivity detector.

in fat and water (a_f, a_w), the density of body fat (ρf), and the fraction of body weight that is fat and water (f_f, f_w). K is measured experimentally by integrating the ($F\dot{Q}/W$) curve from time zero to infinity, neglecting the pulmonary contribution. A plot of K vs. body weight indicates that there is no statistical dependence on W (Table II). However, Figure 12 shows that τ, the time constant, is related to body weight. The time constants in these experiments are much shorter than the longest time constant determined in the dose–response experiments (25.5 minutes).

Discussion

The time-based dose–response curve yielded a slow tissue time constant of 25.5 minutes. This is significantly greater than any circulation time constants previously reported in small animals (7). The experiments cannot indicate the anatomical location or the mode of transport responsible for this slow time constant. Flynn's studies (7), which failed to show such a slow tissue, were performed on unanaesthetized mice so the conditions for comparison are not exact. Detection of this slow tissue by measurement of pulmonary gas washout is probably not feasible be-

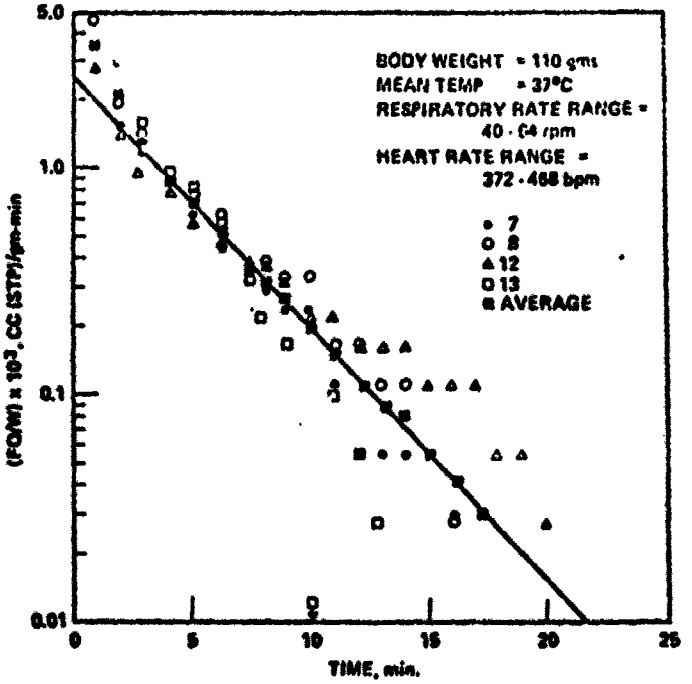

Figure 11. Exhaled N_2 $\frac{FQ}{W}$ as a function of time

Washout data from four, 110-gram hamsters with a mean body temperature of 37°C. The arithmetic average points (⊡) describe a simple exponential function of time.

Table I. Slope (τ) and Intercept ($FQ/W \times 10^4$) of Washout Curves

Total Body Weight, grams	τ, *minutes*	$(FQ/W \times 10^4)$, *cc/g-min*
75	.542	33.5
85	.875	25.0
88	.748	17.5
93	1.31	18.8
102	1.48	24.8
107	1.63	20.3
110	1.37	18.3
121	1.86	17.0

cause of the extremely low quantity of N_2 involved and the many sources of N_2 leaks that could yield this much nitrogen (diffusion through plastic tubing, transcutaneous N_2 transport, or leaks around seals).

If one extrapolates the pressure-based dose–response data to a 1% mortality level (a threshold for the disease), the inert gas partial pressure is 2.5 ata. Trials on humans have indicated a critical threshold for detecting decompression sickness at 2 ata, not too different from the value for

Table II. Experimental Values of $K \times 10^3$

Total Body Weight, grams	$K \times 10^3$, *cc/g-atm*
75	2.33
85	2.80
88	1.67
93	3.16
102	4.70
107	4.23
110	3.22
121	4.05

hamsters. This would imply that the population response curves for type 2 symptoms as measured on hamsters is not too different from the response curves for humans with type 1 symptoms at the low incidence level. This then suggests that the curves drawn in Figure 4 would be virtually coincident at the lower response levels. It is just this tendency for the curves to coincide that makes it so difficult to settle the arguments concerning the presence or absence of asymptomatic bubbles in human divers.

Figure 9 indicates that the slow tissue that was responsible for mortality in saturation dives could not be responsible for the high mor-

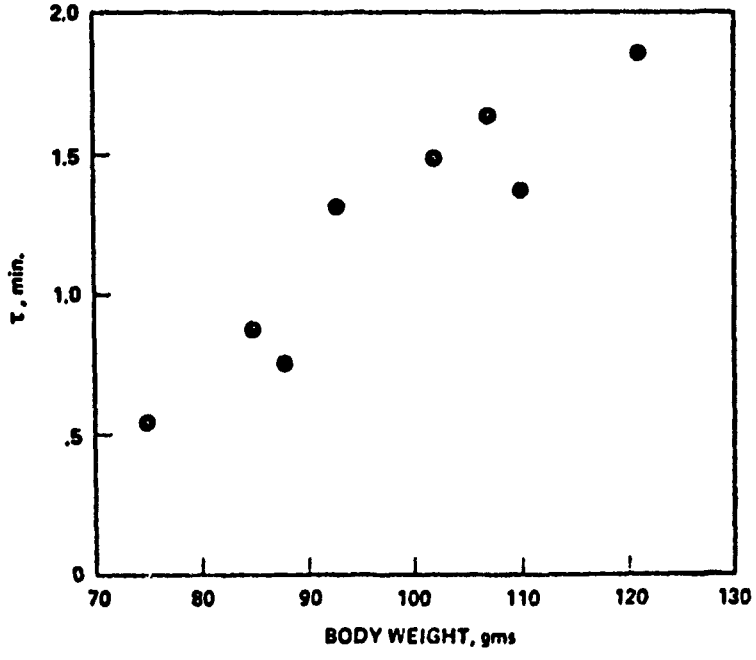

Figure 12. N, washout time constant (τ) as a function of body weight

tality in the shorter dives. That is, the experimental mortality was significantly greater than the least-squares line based on the slow tissue. One explanation of this would be that faster time constant tissues exist in the body and are responsible for the higher mortality in the shorter dives. Since we know from the N_2 washout studies that faster tissues do exist, it is worth trying to determine whether these faster tissues could be sites of nucleation for short dives.

If we assume that all tissues have the same susceptibility to bubble formation, their inert gas tissue tension should be the same as the best experimental line for the PB data. By this method we can calculate back to determine what the time constant of these faster tissues would be in order to acquire this level of inert gas tension. When this is done, the tissue time constant is 6.3 minutes for the two-minute bottom time experiments. While this is significantly faster than the 25.5-minute constant measured for the slow tissues, it is still significantly greater than the slowest time constant measured in the nitrogen washout studies (Figure 12). Thus, it is assumed that the well-perfused tissues of the body would never be the sites of bubble formation for dives greater than two minutes. These data also confirm experimentally the generally held notion that there is a spectrum of response time for the body tissues.

A range of physiologic responses was noted in hamsters exposed to the washout studies. Core temperatures as low as 30°C were measured. Heart rates ranged from 324 to 564 cpm, and respiration rates were 40–68 rpm. In spite of this, no significant systematic variation of time constants could be demonstrated. This is interpreted to mean that the time constants measured by this technique are for tissues that are so well perfused that they are independent of variabilities in the physiologic parameters measured. Peripheral tissues that are known to be sensitive to these parameters are obviously not measured by this method.

A comparison of the experimentally measured K value (Table II) and various theoretical K values is instructive. An average 100-gram hamster is 63.4% water, 17.4% fat, and 19.2% bone and other material (kindly determined by F. K. Millar, Laboratory of Physiology, NCI, NIH, Bethesda, Md.). Based on published values of solubility coefficients, one can compute a theoretical value of K of 26.2×10^{-3}. Thus, we must infer that only part of the total nitrogen washout was actually measured during the washout studies. At the other extreme, one could assume that we measured only the nitrogen dissolved in the bloodstream. When the average K value is converted to a fractional composition, assumed to be water, the fraction is 0.13. This is significantly higher than the known factor of blood (~.07) and much lower than the total water content. Thus, we must be measuring some volume greater than

the blood volume. It is inferred that certain tissues are perfused in an equilibrium fashion with the blood and are, therefore, washed out at the same rate as is the blood.

Various ways have been used to estimate the cardiac output per gram of tissue of animal species. Since direct information on cardiac output for hamsters is not available, different estimation procedures were used. These are summarized in Appendix III. The average value of cardiac output per gram of tissue is 0.64 cc/gram-min, based on a 100-gram hamster. Notice from Figure 11 that the inverse of the cardiac output per gram of tissue (1.6 minutes) is similar to the time constant for a 100-gram hamster. This lends strong credence to the observation above that the time constant measured for gas washout from hamsters in these experiments is essentially that of the gas dissolved in blood and the well perfused tissues of the body.

Summary

Arguments are presented that favor a four-tissue model of a hamster from an inert gas exchange point of view; (1) lung, (2) a fast tissue with a time constant corresponding to the cardiac output per gram of tissue, and (3,4) two slow tissues (time constant 6.3 and 25.5 minutes) corresponding to those tissue sites susceptible to bubble nucleation.

Acknowledgments

We express our appreciation for technical assistance in these experiments of L. Hardy, D. Bennett, L. Sutermeister, and J. M. Miles, Jr. F. K. Millar who graciously assisted us in determining hamster body composition.

Appendix I—Analysis of Time-Based Data by the Method of Probits

It is assumed that the time-based data fit a theoretical dose–response curve as shown in Figure 6. Analysis of such dose–response curves, first described by Bliss (*10*), consists of finding a convenient method to linearize the data. In such a linearized form, a least-squares regression line and standard estimates of data variance can be obtained.

However, the data are generally too sparse to permit simple analysis. Some judgment must be made of the several possible results to obtain one that is internally consistent. An example of this procedure is given here for the time-based data. The data are presented in Table I-A.

Table I-A. Time-Based Data

Bottom Time, min.	n	*Mortality, %*
2	80	2.50
4	80	8.75
8	80	12.50
16	80	25.0
31	289	52.9
90	80	63.75

The data are converted to the coordinate system of probits as a function of log (time). First the mortality data must be converted to response data. One may do this with one of two plausible assumptions: (a) that the mortality at 90 minutes corresponds to 100% response, or (b) that the mortality at both 31 and 90 minutes corresponds to 100% response, and one then lumps the data. The mortality data are converted to response data by expressing each as a percentage of the mortality selected as the 100% response. These data are plotted against the $\log_{10}$ (time). Data based on the two assumptions are given in Table I-B.

Table I-B. TB Data Expressed as Response Data

Bottom Time, min.	$\log_{10}$ *(time)*	% *Response (a)*	*Probit (a)*	% *Response (b)*	*Probit (b)*
2	.301	3.91	3.24	4.27	3.28
4	.602	13.7	3.90	15.0	3.96
8	.903	19.6	4.14	21.4	4.21
16	1.204	39.2	4.73	42.7	4.81
31	1.491	83.0	6.15	100.0	—
90	1.959	100.0	—	100.0	—

Although the data do not appear too different, logic leads us to select assumption (a). An approximate best fit to the data yields a time constant of about 30 minutes. If this is true, the data points of 31 minutes could not be at all representative of saturation data.

Since the data exhibits significant scatter, one must use a least-squares method to correlate probit with $\log_{10}$ (time) [*see* Finney (9), Chapter 4]. This is done in an iterative style of successively improving the approximation to the least-squares line. Four iterations were required to yield a least-squares lines given by:

$$\text{Probit} = 2.08 + 2.54 \log_{10} (\text{time})$$

A 99% response occurs when probit = 7.326. This yields a t_{99} (time when 99% response occurs) given by: t_{99} = antilog$_{10}$ (2.068) = 117 minutes.

Since we have assumed that this level of mortality is produced by a slow tissue reaching saturation with N_2 along an exponential curve, $e^{-t/\tau}$, the time constant is related to t_{50} by:

$$\tau = t_{50} \div 4.61$$

Thus, $\tau = 25.5$ minutes.

Appendix II—Analysis of Nitrogen Washout Data

The nitrogen washout data consist of F, the fraction of nitrogen in exhaled air, measured as a discrete function of time after shifting to an 80–20 He–O_2 breathing mixture. When plotted as log F vs. time, the data fall along one line. Only the first one or two data points are above this "best" line. These presumably are caused by pulmonary and breathing loop dead spaces and are neglected hereafter.

To a first approximation:

$$[\text{Total } N_2 \text{ excreted}]\ t = n\Delta t = \sum_{j=1}^{n} F_j \dot{Q}_j \Delta t$$

where $\dot{Q}_j$ is the gas flow rate during the interval F_j is measured. When $n = \infty$, the total nitrogen excreted should equal the total nitrogen dissolved in the body at the start of the experiment (neglect skin transport of N_2 for this analysis). That is

$$V_{N_2\text{-TOT}} = \sum_{j=1}^{\infty} F_j \dot{Q}_j \Delta t = (V_f \alpha_f + V_w \alpha_w) P_{N_2\text{-air}}$$

where V_f (or V_w) is the volume of fat (or water) and α_f (or α_w) is the solubility coefficient for N_2 in fat (or water). This expression may be rewritten as:

$$V_{N_2\text{-TOT}} = W_{TOT} K P_{N_2\text{-air}}$$

where,

$$K = \left[\frac{f_f \alpha_f}{\rho_f} + f_w \alpha_w\right]$$

ρ_f is the density of fat, and f is the weight fraction of fat or water.

Since we do not have data for $F\dot{Q}$ to infinity, it seemed desirable to derive a mathematical expression for it so as to convert the summation

to an integration. Consider the body as a lumped mass that transmits N_2 to the breathing loop at a rate

$$\dot{q} = k\overline{P}$$

where $\overline{P}$ is mean body N_2 partial pressure, and k is a transfer coefficient, and $\dot{q}$ is the nitrogen excretion rate.

Now,

$$\dot{q} = \frac{d}{dt}(V_{N_2\text{-}TOT}) = \frac{d}{dt}(KW_{TOT}\overline{P})$$

Rearranging,

$$\frac{k}{KW_{TOT}} = \frac{d\ln\overline{P}}{dt}$$

It is also true that $F = q/\dot{Q}$ if one can neglect variations in q_{O_2}, q_{CO_2}, and q_{H_2O}.

From this we obtain,

$$F = \frac{k}{\dot{Q}}\overline{P}$$

so,

$$\frac{dF}{dt} = \frac{k}{\dot{Q}}\frac{d\overline{P}}{dt}$$

and

$$\frac{1}{F}\cdot\frac{dF}{dt} = \frac{1}{\overline{P}}\frac{d\overline{P}}{dt}$$

Thus,

$$\frac{d\ln F}{dt} = \frac{k}{KW_{TOT}}$$

Note also that: $\dfrac{d\ln(F\dot{Q}/KW_{TOT})}{dt} = \dfrac{d\ln\overline{P}}{dt}$

Hence, the slope of a line plotted through the data (log $(F\dot{Q}/KW_{TOT})$ *vs.* time) will yield a whole body mass transfer coefficient. It will then be possible to compute the experimental value of K by simple integration.

Appendix III—Estimation of Hamster Cardiac Output

Several methods are used to estimate cardiac output (CO), with data gathered from various animal species. Each is described, then an average value is taken. All data are based on a 100-gram hamster.

(A) $CO = \frac{(\text{Blood Volume})}{(\text{Circulation Time})}$

Blood volume $= f_B W_{TOT} = .074 \times 100 = 7.4$ cc
Circulation time: (Ref. *11*, p. 115)
man: 7–9 sec
dog: 10–11 sec
rabbit: 10.5 sec
If we assume for a hamster it is 10 sec, CO = 44.4 cc/min.

(B) CO = (Cardiac Index) × (Surface Area)

Cardiac index $= 1.6 \times 10^{-3}$ cc/min-sq m (Rat, Ref. *11*, p. 80)
Surface area $= .091 \times W_{TOT}^{2/3}$ (Rat, Ref. *11*, p. 80)
CO = 31.5 cc/min

(C) CO = (Cardiac Index) × (Surface Area)

Cardiac index $= 2.47 \times 10^3$ cc/min-in^2 [anesthetized ferret, (*12*)]
Surface area $= .061\ W_{TOT}^{2/3}$
CO = 53.2 cc/min

(D) $CO = \frac{(\text{Blood Volume})}{(\text{Circulation Time})}$

Blood volume = 7.4 cc (*see* III A)
Circulation time = 4.5 sec (*see* III C)
CO = 98.7

(E) $CO = \frac{(O_2 \text{ Consumption})}{(A\text{-}V\ O_2 \text{ Gradient})}$

O_2 Consumption = 2.3 cc/gram-hr (*see* III A)
A-V O_2 Gradient = 4.1 vol % [anesthetized dogs (*13*)]
CO = 98.7 cc/min

(F) The arithmetic average cardiac output is 64.3 cc/min. No weighing is given the various estimates because of uncertainties in all methods.

Literature Cited

1. Haldane, J. S. *et al.*, *J. Hygiene* (1908) **8**, 342.
2. Workman, R. D., "American Decompression Theory and Practice," in "The Physiology and Medicine of Diving and Compressed Air Work," P. B. Bennett, D. H. Elliott, Eds., pp. 252–290, Williams and Wilkins, Baltimore, 1969.
3. Bischoff, K. B. *et al.*, *Cancer Chemotherapy Repts. Pt. 1* (April 1970) **54** (2).
4. Oyama, Y., Spencer, M. P., *Physiologist* (1969) **12**, 320.
5. Gillis, M. F. *et al.*, *Nature* (March 1968) **217**, 965–967.
6. Smith, Kent H., Johanson, Dave, Virginia Mason Research Institute (Seattle, Wash.), *Tech. Rept.*, ONR Cont. N00014-69-C-0402 (1 June 1970).

7. Flynn, E. T., Lambertson, C. J., "Underwater Physiology," pp. 179–191, Academic, New York, 1971.
8. Buckles, R. G., Hardenbergh, E., *Proc. Intern. Congr. Hyperbaric Medicine, 4th, Tokyo* (1970), 109–115 (Igaku Shain Ltd.)
9. Finney, D. J., "Probit Analysis—A Statistical Treatment of the Sigmoid Response Curve," University Press, 1952
10. Bliss, C. I., *Science* (1934) 79, 38–39.
11. "Handbook of Circulation," WADC TR59-593.
12. *Proc. Soc. Exp. Biol. Med.* (1949) 72, 711–714.
13. "Handbook of Respiration," WADC TR58-352, p. 58.

RECEIVED December 8, 1971. Studies carried out at the Naval Medical Research Institute National Naval Medical Center, Bethesda, Md. under support from the Bureau of Medicine and Surgery, Navy Department, Research Task M4306, 01-1020B. The opinions and assertions herein are the authors' alone and do not necessarily reflect the views of the Navy Department or the naval service at large.